Divergent Synthesis of Indolenine and Indoline Ring Systems by Palladium-Catalyzed Asymmetric Dearomatization of Indoles

Dong Gao and Prof. Dr. Lei Jiao*

Abstract: Dearomatized indole derivatives bearing a C3- or C2-stereocenter exist ubiquitously in natural products and biologically active molecules. Despite remarkable advances in their synthesis, stereoselective and regio-divergent methods are still in a high demand. Herein, a Pd-catalyzed intermolecular asymmetric spiroannulation of 2,3-disubstituted indoles with internal alkynes has been developed for the efficient construction of indoline structures with a C2-quaternary stereocenter. Stereospecific aza-semipinacol rearrangement of these indoline derivatives under acidic conditions afforded indolenine products bearing a C3-quaternary stereocenter, where the migrating group could be controlled by the reaction sequence. The asymmetric spiroannulation together with the subsequent aza-semipinacol rearrangement enabled a divergent access to dearomatized indole derivatives with either a C3- or a C2-quaternary stereocenter.

Indolenines bearing a C3-quaternary stereocenter and indolines bearing a C2-quaternary stereocenter are widely occurring core structures in many natural products and biologically active molecules,[1,2b,2d] and the synthetic methods that enable efficient construction of these core structures is highly demanded.[2] Catalytic asymmetric dearomatization (CADA) reactions serve as one of the most straightforward approach to chiral building blocks from aromatic substrates.[3] Recently, a series of CADA reactions have been developed for the construction of chiral indolenine/indoline derivatives based on the reactivity of C(sp^2)-Pd species (Scheme 1).[4-6] The majority of these reactions were performed in an intramoleculcar manner (Scheme 1a), in which a haloarene or an acetylene is tethered to the N1-, C2- or C3-position of indole as the C(sp^2)-Pd precursor. The You group achieved enantioselective C3-arylation of C3-tethered indoles;[4p] Jia[4b,4k] and Fukuyama[4n] developed the dearomative Heck reaction of N1- and C2-tethered indoles to build a C2-stereocenter; Jia,[4h-j,4m,4o] Liang,[4c,4d,4g] Lautens,[4h] and Dai[4e] reported the asymmetric dearomative difunctionalization of C2-tethered indoles by employing an external nucleophile.

Compared with intramolecular cyclization, the intermolecular version allows for a more divergent approach to dearomatized products. In this regard, Zhang and co-workers reported recently an enantioselective annulative dearomatization of C3-bromoarylindoles with alkynes using the Pd/Sadphos catalytic system to access various spiro-indolenines with a C3-quaternary stereocenter (Scheme 1b).[5] However, to date the intermolecular asymmetric dearomatization of C2-arylindoles has not been reported yet, and stereoselective construction of structurally diversified indoline/indolenine derivatives remains a formidable challenge.[7]

Herein, we report a Pd-catalyzed asymmetric intermolecular spiroannulation reaction of C2-arylindoles with internal alkynes, leading to the formation of spiro-indolines bearing a C2-quaternary stereocenter (Scheme 1c). These products could undergo a stereospecific aza-semipinacol rearrangement under acidic conditions, affording fused-indolenines with a C3-quaternary stereocenter. Furthermore, the migration selectivity of this process could be tuned by the selection of reaction sequence. The asymmetric spiroannulation together with the stereospecific rearrangement enabled a divergent access to dearomatized indole derivatives with either a C3- or a C2-quaternary stereocenter.

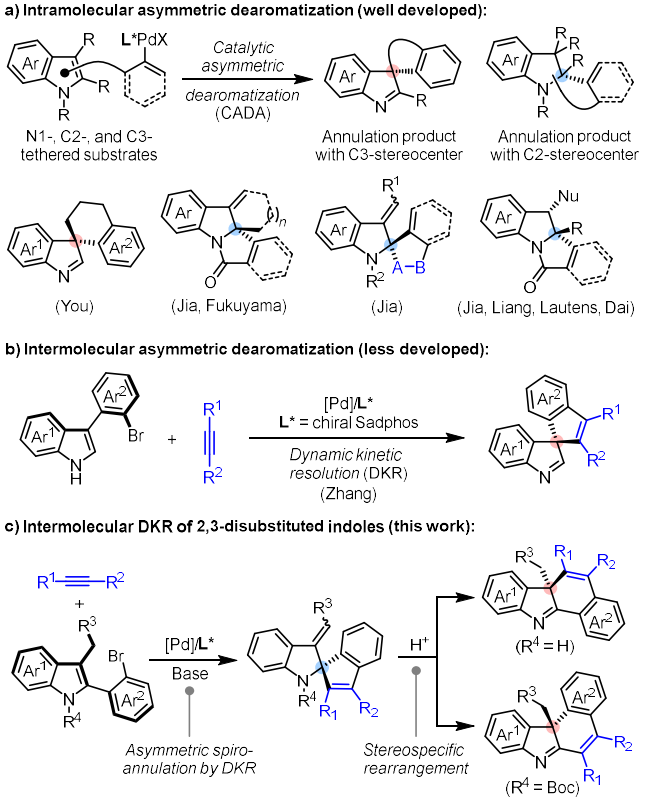

Scheme 1. Palladium-Catalyzed Asymmetric Dearomatization of Indoles Involving a C(sp^2)-Pd Species.

At the outset, we envisioned to attempt the reaction between Boc-protected 2-(2-bromophenyl)-3-methyl-1*H*-indole (**1a**) and alkynes as a model reaction. We first focused on the aryl-aryl rotational barrier of **1a**, since similar substrates exhibit axial chirality[5,6d] and facile interconversion between the two enantiomers is crucial for efficient dynamic kinetic resolution (DKR).[8] We found that, the enantiomers of **1a** could be well resolved by chiral HPLC, indicating that they interconvert slowly under room temperature (Scheme 2). The separation of both enantiomers allowed us to determine the kinetic parameters of the racemization process by performing the reaction under elevated temperatures.[9] On the basis of the measured enantiomerization rate constants, the enantiomerization barrier of **1a** was determined to be 25.4 kcal/mol at 298 K by applying the Erying equation, which ensures a rapid racemization process at elevated temperature.

[*] D. Gao, Prof. Dr. L. Jiao
Center of Basic Molecular Science (CBMS), Department of Chemistry, Tsinghua University, Beijing 100084, China
E-mail: Leijiao@mail.tsinghua.edu.cn

Supporting information for this article is given via a link at the end of the document.

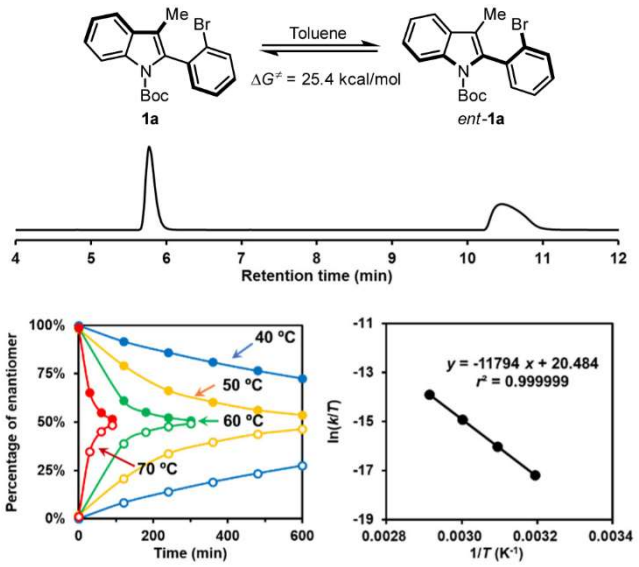

Scheme 2. Rotational Barrier Determination for Substrate **1a**

Bearing this information in mind, we commenced the study on the reaction between **1a** and diphenylacetylene (**2a**) by employing $Pd(dba)_2$ as the precatalyst and toluene as the solvent (Table 1). It was found that, chiral NHC ligand **L1**, BINAP (**L2**), spiro-phosphoramidite ligand **L3**, and Feringa-type ligand **L4** resulted in unsatisfactory results (entries 1-4). To our delight, a promising result was observed by employing the Carreira ligand **L5** with *t*-BuOLi as the base at 120 °C, affording product **3aa** in 55% NMR yield with 92:8 er (entry 5). A better result was achieved by lowering the reaction temperature to 90 °C and switching the base to MeOLi, providing **3aa** in 88% isolated yield with 95:5 er (entry 9). Further optimization on ligand structure indicated that more sterically hindered ligands **L6** and **L7** exhibited a negative effect on enantioselectivity (entries 10-11). The fluoro-substituted ligand **L8** was found to give comparable yield and slightly inferior enantioselectivity (entry 12). A comparison showed that phosphoramidite ligand **L9** was inferior compared with **L5** (entry 13). A brief screen of the *N*-protecting group on indole indicated that the Boc group was the best amongst tosyl, acetyl, and methyl group (entries 14-16).

To illustrate the generality of the reaction, the scope of the indole coupling partners was initially investigated (Table 2). Gratifyingly, 2-aryl-3-methylindole substrates with fluoro, chloro, methoxyl, and methyl substituents (**1b-e**) at the 5-position of the phenyl ring worked well under the optimal reaction conditions, giving the corresponding spiro-indoline products **3ba-3ea** in 70-86% yield with 90:10 to 96:4 er. Substrate bearing an electron-withdrawing trifluoromethyl group (**1f**) was also tolerated to afford **3fa** in 92:8 er, whereas the reaction yield decreased to 23%. 6-Methyl and 4,5-methylenedioxy substituent on the phenyl ring (**1g-h**) and a more sterically congested naphthyl group in place of the phenyl group (**1i**) were tolerated to provide the desired products **3ga-3ia** in 39-99% yield with 93:7-95:5 er. However, introduction of a methyl group at the 6-position (**1j**) of the phenyl moiety resulted in decreased enantioselectivity. Substituents on the indole moiety (5'-methyl, 5'-trifluoromethyl, 5'-chloro, and 4'-chloro) of the substrates (**1k-n**) were compatible with the reaction, delivering **3ka-3na** in 33-82% yield with 93:7-95:5 er, while the 7'-fluoro substituent significantly decreased the yield of the desired product **3oa**. The use of 2-aryl-3-ethylindole substrate **1p** led to a good yield of spiroannulation product **3pa** as a C=C bond geometrical isomer mixture with diminished enantioselectivity.

Table 1. Optimization of the reaction conditions.

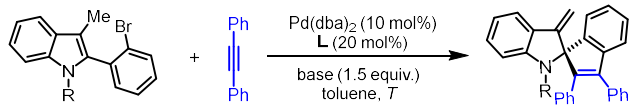

1a: R = Boc, **1a'**: R = Ts
1a'': R = Ac, **1a'''**: R = Me
2a (1.5 equiv.)

Entry	Sub	Base	L	*T*/°C	Yield(%)[a]	Er[b]
1[c]	**1a**	*t*-BuONa	**L1**	120	9	53.5:46.5
2[d]	**1a**	Cs_2CO_3	**L1**	120	23	51.5:48.5
2[e]	**1a**	Cs_2CO_3	**L2**	120	0	-
3[f]	**1a**	*t*-BuOLi	**L3**	120	75	54:46
4[g]	**1a**	*t*-BuOLi	**L4**	120	12	75.5:24.5
5	**1a**	*t*-BuOLi	**L5**	120	55	92:8
6	**1a**	*i*-PrOLi	**L5**	120	60	92:8
7	**1a**	MeOLi	**L5**	120	65	93:8
8[h]	**1a**	MeOLi	**L5**	100	70	95:5
9[i]	**1a**	MeOLi	**L5**	90	88	95:5
10	**1a**	MeOLi	**L6**	95	52	44:56
11	**1a**	MeOLi	**L7**	95	20	46:54
12[i]	**1a**	MeOLi	**L8**	90	89	92:8
13[g]	**1a**	*t*-BuOLi	**L9**	120	52	54.5:45.5
14	**1a'**	MeOLi	**L5**	90	36[i]	62:38
15	**1a''**	MeOLi	**L5**	90	n.d.[j]	-
16	**1a'''**	MeOLi	**L5**	90	n.d.[j]	-

[a] Determined by ^1H NMR with CH_2Br_2 (0.1 mmol) as an internal standard. [b] Enantiomeric ratios were determined by chiral stationary phase HPLC.The absolute configuration of **3aa** was confirmed by the single crystal X-ray diffraction analysis. [c] Using $Pd(OAc)_2$ (10 mol%) as palladium source, KI (1.5 equiv) as additive, and Dioxane (0.1 M) as the solvent. [d] Using $[Pd(C_3H_5)Cl]_2$ (5 mol%) as palladium source, **L1** (15 mol%), and Dioxane (0.1 M) as the solvent. [e] Using $[Pd(C_3H_5)Cl]_2$ (2.5 mol%) and **L2** (7.5 mol%). [f] Using $Pd(dba)_2$ (5.0 mol%) and **L3** (7.5 mol%). [g] Using $Pd(dba)_2$ (10.0 mol%) and **L4** (15.0 mol%). [h] MeOH (1.0 equiv.) as additive. [i] Yield of isolated product. [j] Not detected.

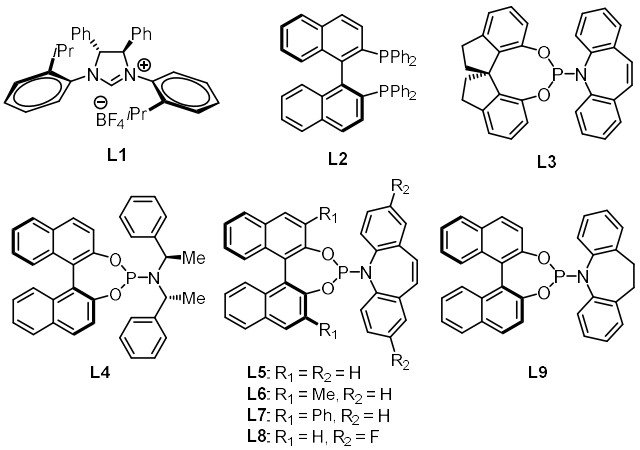

Table 2. Scope of indole substrates and internal alkynes[a]

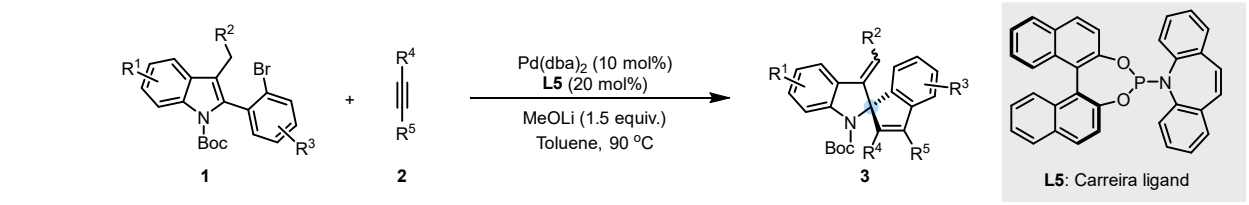

Scope of indole substrate

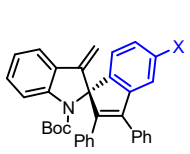

3aa, X = H, 88% yield, 95:5 er
3ba, X = F, 86% yield, 96:4 er
3ca, X = Cl, 73% yield, 96:4 er
3da, X = OMe, 70% yield, 90:10 er
3ea, X = Me, 86% yield, 94:6 er
3fa, X = CF_3, 23% yield, 92:8 er

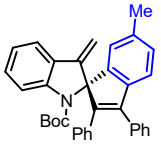

3ga
87% yield, 95:5 er

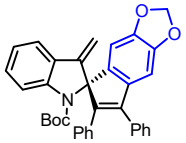

3ha
99% yield, 95:5 er

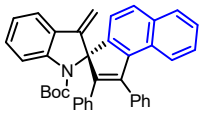

3ia
39% yield, 93:7 er

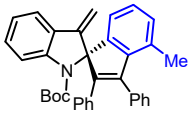

3ja
62% yield, 76:24 er

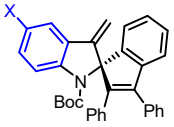

3ka, X = Me, 82% yield, 93:7 er
3la, X = CF_3, 33% yield, 94:6 er
3ma, X = Cl, 59% yield, 93:7 er

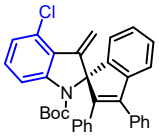

3na
64% yield, 95:5 er

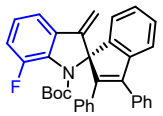

3oa
23% yield, 87:13 er

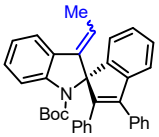

3pa
79% yield, *Z*/*E* = 1:2
(*Z*)-**3pa**: 67.5:32.5 er
(*E*)-**3pa**: 75.5:24.5 er

Scope of alkyne component

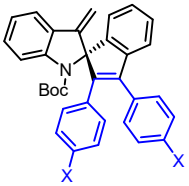

3ab, X = F, 96% yield, 94:6 er
3ac, X = Cl, 74% yield, 93.5:6.5 er
3ad, X = OMe, 97% yield, 94:6 er
3ae, X = CF_3, 57% yield, 92:8 er

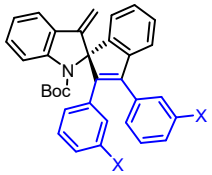

3af, X = F, 94% yield, 91.5:8.5 er
3ag, X = OMe, 93% yield, 95:5 er

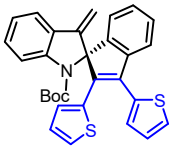

3ah
16% yield, 91:9 er

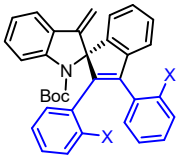

3ai, X = F, 46% yield, 77:23 er
3aj, X = Me, 0% yield

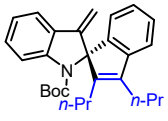

3ak
91% yield, 92:8 er
[98%, 90:10 er on 1.3 g scale]

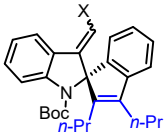

3pk, X = Me
95% yield, *Z*/*E* = 1:12
(*Z*)-**3pk**: 90:10 er
(*E*)-**3pk**: 88:12 er

3qk, X = $CO_2{}^t$Bu
55% yield, *Z*/*E* = 1:12
(*Z*)-**3qk**: 83:17 er
(*E*)-**3qk**: 88:12 er

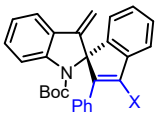

3al-3am

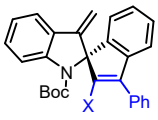

3al'-3am'

3al/3al', X = CH_2OTBS
3al, 78% yield, 94:6 er
3al', 16% yield, 93.5:6.5 er

3am/3am', X = Me
3am, 83% yield, 89:11 er
3am', 15% yield, 77:23 er

Benzofuran substrate

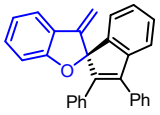

3ra
30% yield, 83.5:16.5 er[b]

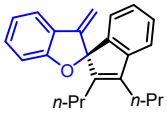

3rk
93% yield, 89:11 er[b]

[a] Reaction conditions: **1** (1.0 equiv), **2** (1.5 equiv), and toluene (0.1 M) under Ar. Yields of isolated products are reported. The *Z*/*E* ratios were determined by crude ^{1}H NMR. The er values were determined by chiral HPLC. [b] **L4** (20 mol%) was used in place of **L5**.

Then the scope of the internal alkyne was explored (Table 2). Symmetrical diaryl acetylenes with various substituents at the *para*- (**2b-e**) or *meta*- (**2f-g**) position of both phenyl rings participated in the reaction smoothly to give the corresponding products **3ab-3ag** in 57-97% yield with 92:8-95:5 er. Di(thiophen-2-yl)acetylene (**2h**) could undergo the reaction with **1a**, but afforded a low yield of cyclization product **3ah** in 91:9 er. The *ortho*-substituent on the aryl groups of diarylacetylene generally exhibited a negative effect on the reaction: *ortho*-fluoro substituted 1,2-bis(2-fluorophenyl)ethyne **2i** afforded product **3ai** in a moderate yield with a low enantioselectivity (77:23 er), and no desired product was observed for the more sterically hindered *ortho*-methyl substituted diphenylacetylene **2j**. To our delight, the symmetrical dipropylacetylene **2k** was found to be suitable to undergo the annulation with substrates **1a**, **1p**, and **1q**. Notably, a gram-scale synthesis of **3ak** (1.31 g) was carried out to afford the product in 98% yield with 90:10 er, indicating the scalability of the present method. Moreover, the reactions of 2-aryl-3-ethylindole substrate **1p** and 2-aryl-3-*tert*-butoxycarbonylmethylindole substrate **1q** with alkyne **2k**

afforded the corresponding products **3pk** and **3qk** in good yields and enantioselectivities. Finally, the unsymmetrical alkyl/aryl mixed acetylenes **2l** and **2m** produced cyclization products in good yields with decent enantioselectivities and satisfactory regioselectivities.

Interestingly, we found that the present protocol could be extended to a 2-aryl-3-methylbenzofuran substrate by employing **L4** as the ligand, affording spiro[benzofuran-cyclopentane] **3ra** and **3rk** in comparable enantioselectivities.

The C2-spiroindoline structure in the cyclized products enabled a potential aza-semipinacol rearrangement[4f, 10] leading to the formation of a C3-stereocenter, and if the rearrangement proceeded stereospeficially, enantioenriched C3-substituted indolenine derivative could be obtained. Therefore, we attempted to perform an acid-promoted aza-semipinacol rearrangement on the spiroindoline products (Table 3). We found that, by treating the C3-methylene (**3aa**, **3aj**, **3am**) or C3-ethylidene (**3pj**) substituted spiro-indolines with TFA (Condition A), the rearranged products bearing a C3-quaternary stereocenter (**4aa**, **4aj**, **4am**, and **4pj**) were obtained in moderate to excellent overall yield without loss of enantiopurities. In this process both the cleavage of the *N*-Boc group and the stereospecific rearrangement of the C2-substituent proceeded smoothly, and the aryl migration was favored over the alkenyl migration.

To figure out whether the rearrangement step occurs prior to or after the elimination of the *N*-Boc group, we investigated another reaction sequence involving stepwise deprotection and rearrangement for the same set of C2-spiroindoline derivatives (Condition B). The deprotection of *N*-Boc group proceeded smoothly by treatment with TMSOTf/2,6-lutidine, and the crude deprotected product was treated with TFA as before. To our surprise, this reaction sequence delivered alkenyl migration product (**4aa'**, **4aj'**, **4am'**, **4pj'**) as the major product with complete retention of enantiopurities. This result indicates that the nature of the *N*-substituent has a remarkable effect on the aza-semipinacol rearrangement, and under Condition A the rearrangement occurred prior to deprotection. Therefore, by choosing an appropriate reaction sequence, rearrange of C2-spiroindoline to C3-substituted indolenine with selective aryl/alkenyl migration could be achieved.

In order to gain more mechanistic insights into the Pd-catalyzed cascade spiroannulation and the regio-divergent aza-semipinacol rearrangement, we performed a DFT computational study (Scheme 3). The reaction between indole **1a** and alkyne **1b** catalyzed by Pd/**L5** was selected as the model, and the calculated reaction pathway is shown in Scheme 3a. It was found that, the reaction starts with the Pd-ligand complex, Pd(**L5**)$_2$,[11] and proceeds through oxidative addition, alkyne coordination and insertion, indole insertion, and β-H elimination steps. The alkyne insertion step via **TS2** turned out to be both turnover-limiting and selectivity-determining, and the overall activation barrier for the formation of **3aa** was 20.4 kcal/mol in terms of Gibbs free energy. The other pathway leading to *ent*-**3aa** starts from the coordination of *ent*-**1a** with the Pd catalyst, and the key alkyne insertion step via **TS2'** was less favored by 1.1 kcal/mol compared with **TS2**, in agreement with the preference for (*R*)-product observed experimentally. It is notable that the barrier for the interconversion of atropisomers of **1a** ($\Delta G^{\neq}$ = 25.4 kcal/mol) seemed to be higher than that for the catalytic dearomatization via **TS2** ($\Delta G^{\neq}$ = 20.4 kcal/mol). Given that **TS2** involves three components (catalyst, substrate **1a**, and alkyne **2a** at 0.01 M, 0.1 M, and 0.15 M, respectively), the corrected barrier for the dearomatization reaction ($\Delta G^{\neq}$ = 25.6 kcal/mol) fits the requirement for DKR. The fact that unconsumed **1a** was determined to be racemic at different conversions confirmed the DKR scenario experimentally (see the Supporting Information for details).

Table 3. Aza-semipinacol rearrangement[a]

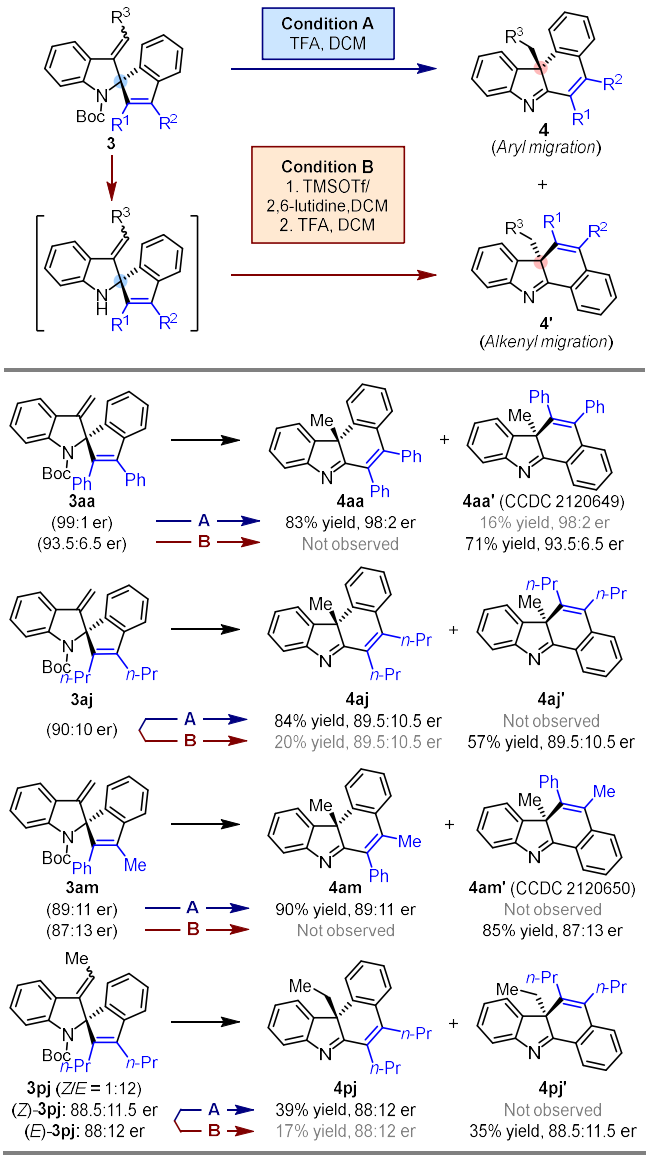

[a] Condition A: TFA/DCM = (1:10 v/v) (0.1 M). Condition B: 1. TMSOTf (4.0 equiv), 2,6-lutidine (5.0 equiv), DCM (0.1 M) 2. TFA/DCM = (1:10 v/v) (0.1 M). Yields of isolated product are reported. The *er* values were determined by chiral HPLC. TFA = trifluoroacetic acid, TMSOTf = trimethylsilyl trifluoromethanesulphonate.

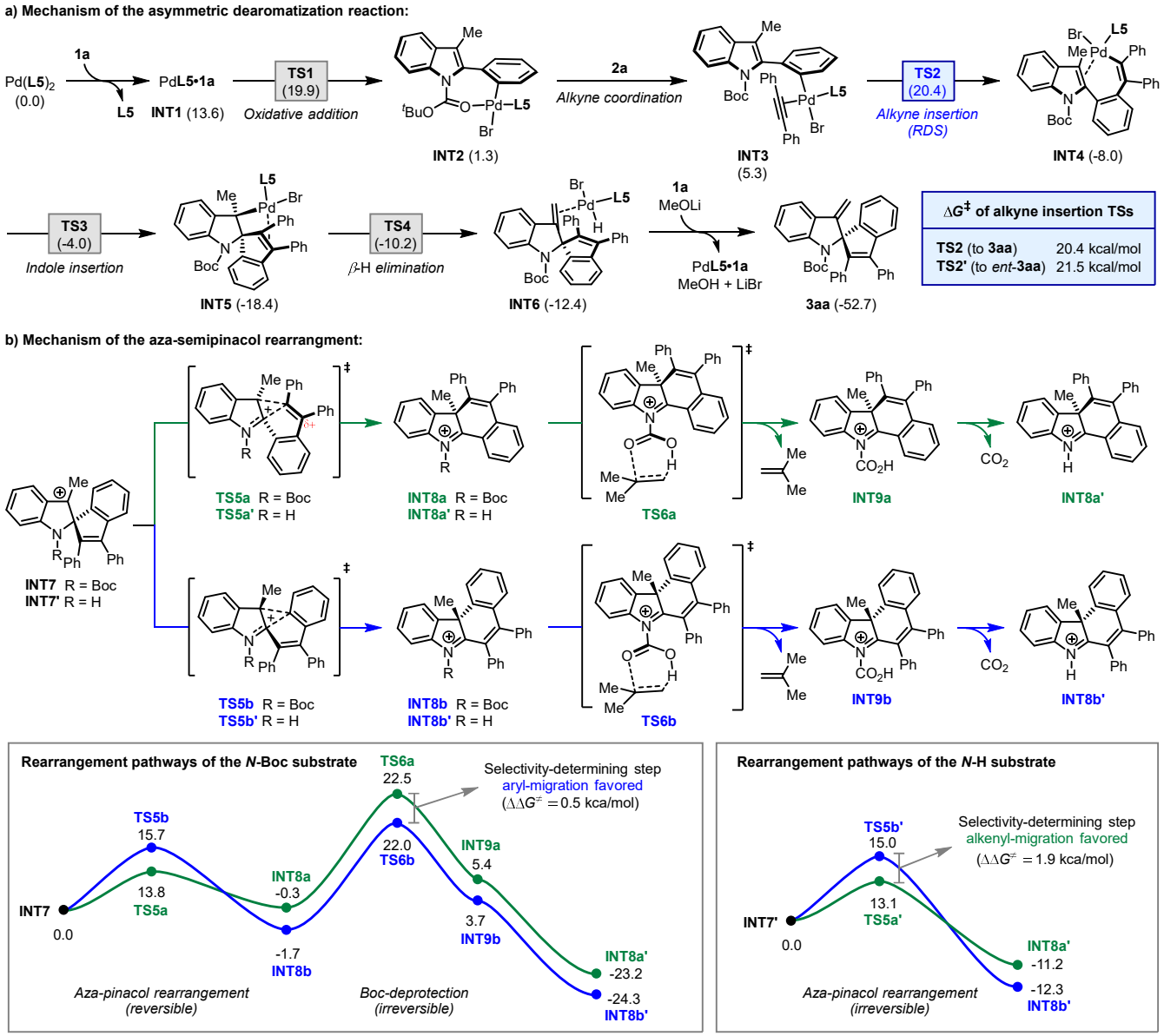

Scheme 3. DFT Computational Study on the Reaction Mechanism. Calculated Gibbs free energies in solution (in kcal/mol) are provided.

The aza-semipinacol rearrangement was also investigated by DFT calculation to understand the nature of the migration selectivity, employing the transformation of **3aa** to **4aa** and **4aa'** as the model (Scheme 3b). The result indicated the aza-semipinacol rearrangement of both the *N*-Boc substrate (starting from **INT7**) and the *N*-H substrate (starting from **INT7'**) favors alkenyl migration (**TS5a** vs **TS5b** and **TS5a'** vs **TS5b'**). We attribute this trend to the fact that alkenyl migration transition states **TS5a** and **TS5a'** could better stabilize the positive charge due to the existence of the aryl rings, whereas this stabilizing effect lacks in the aryl migration transition states **TS5b** and **TS5b'**. Interestingly, for the *N*-Boc substrate the rearrangement is reversible due to a more energy-demanding Boc-deprotection step, while for the *N*-H substrate the rearrangement is irreversible and thus determines the migration selectivity. As a result, the migration selectivity of the *N*-Boc substrate is dictated by the Boc-deprotection step via **TS6a** and **TS6b,** and the preference for the aryl-migrated product in this step inherits from the thermodynamic stability of the rearranged intermediates **INT8a** and **INT8b**.

In summary, we have developed a palladium-catalyzed enantioselective intermolecular dearomatization of C2-arylindoles with internal alkynes, leading to C2-spiroindolines bearing a C2-quaternary stereocenter with good yields and enantioselectivities. The stereospecific aza-semipinacol rearrangement afforded enantioenriched indolenine derivatives bearing a C3-quaternary stereocenter via an tunable aryl/alkenyl migration. The combined steps enabled a divergent access to dearomatized indole derivatives with either a C3- or a C2-quaternary stereocenter.

Acknowledgements

The National Natural Science Foundation of China (Grant No. 21822304) are acknowledged for financial support. The technology platform of CBMS is acknowledged for providing instrumentation and computational resources.

Keywords: indoles · indolenine · catalytic asymmetric dearomatization · stereospecific rearrangement · palladium catalysis

[1] For representative reviews, see: a) P. Ruiz-Sanchis, S. A. Savina, F. Albericio, M. Álvarez, *Chem. Eur. J.* **2011**, *17*, 1388-1408; b) S.-M. Li, *Nat. Prod. Rep.* **2010**, *27*, 57-78.

[2] For representative reviews and examples, see: a) T. S. Silva, M. T. Rodrigues Jr, H. Santos, L. A. Zeoly, W. P. Almeida, R. C. Barcelos, R. C. Gomes, F. S. Fernandes, F. Coelho, *Tetrahedron* **2019**, *75*, 2063-2097; b) J. Bariwal, L. G. Voskressensky, E. V. Van der Eycken, *Chem. Soc. Rev.* **2018**, *47*, 3831-3848; c) J. Song, D.-F. Chen, L.-Z. Gong, *Natl. Sci. Rev.* **2017**, *4*, 381-396; d) M. J. James, P. O'Brien, R. J. Taylor, W. P. Unsworth, *Chem. Eur. J.* **2016**, *22*, 2856-2881; e) J. D. Podoll, Y. Liu, L. Chang, S. Walls, W. Wang, X. Wang, *Proc. Natl. Acad. Sci. U. S. A.* **2013**, *110*, 15573-15578; f) M. Bandini, A. Eichholzer, *Angew. Chem. Int. Ed.* **2009**, *48*, 9608-9644; *Angew. Chem.* **2009**, *121*, 9786-9824.

[3] For representative reviews, see: a) C. Zheng, S.-L. You, *ACS Cent. Sci.* **2021**, *7*, 432-444; b) Z. Wang, *Org. Biomol. Chem.* **2020**, *18*, 4354-4370; c) C. Zheng, S.-L. You, *Nat. Prod. Rep.* **2019**, *36*, 1589-1605; d) J. M. Saya, E. Ruijter, R. V. A. Orru, *Chem. Eur. J.* **2019**, *25*, 8916-8935; e) J.-B. Chen, Y.-X. Jia, *Org. Biomol. Chem.* **2017**, *15*, 3550-3567; f) C. Zheng, S.-L. You, *Chem* **2016**, *1*, 830-857; g) W.-T. Wu, L. Zhang, S.-L. You, *Chem. Soc. Rev.* **2016**, *45*, 1570-1580; h) S. P. Roche, J.-J. Youte Tendoung, B. Tréguier, *Tetrahedron* **2015**, *71*, 3549-3591; i) C. X. Zhuo, C. Zheng, S.-L. You, *Acc. Chem. Res.* **2014**, *47*, 2558-2573; j) C. X. Zhuo, W. Zhang, S.-L. You, *Angew. Chem. Int. Ed.* **2012**, *51*, 12662-12686; *Angew. Chem.* **2012**, *124*, 12834-12858; For a book, see: k) S.-L. You, *Asymmetric Dearomatization Reactions,* VCH, Weinheim, **2016**.

[4] For a review, see: a) N. Zeidan, M. Lautens, *Synthesis* **2019**, *51*, 4137-4146. For representative examples, see: b) R.-X. Liang, L.-J. Song, J.-B. Lu, W.-Y. Xu, C. Ding, Y.-X. Jia, *Angew. Chem. Int. Ed.* **2021**, *60*, 7412-7417; *Angew. Chem.* **2020**, *133*, 7488-7493; c) Y. Li, H.-Y. Zhang, Y. Zhang, Y.-P. Han, J. Zhao, Y.-M. Liang, *J. Org. Chem.* **2021**, *86*, 14640-14651; d) Y. Li, Yue-Su, H.-Y. Zhang, Y. Zhang, Dong-Han, Y.-P. Han, J. Zhao, Y.-M. Liang, *ChemistrySelect* **2021**, *6*, 4719-4724; e) M.-L. Han, W. Huang, Y.-W. Liu, M. Liu, H. Xu, H. Xiong, H.-X. Dai, *Org. Lett.* **2021**, *23*, 172-177; f) D. Gao, L. Jiao, *J. Org. Chem.* **2021**, *86*, 5727-5743; g) Z. Zhang, B.-S. Zhang, K.-L. Li, Y. An, C. Liu, X.-Y. Gou, Y.-M. Liang, *J. Org. Chem.* **2020**, *85*, 7817-7839; h) C. Shen, N. Zeidan, Q. Wu, C. B. J. Breuers, R.-R. Liu, Y.-X. Jia, M. Lautens, *Chem. Sci.* **2019**, *10*, 3118-3122; i) R.-X. Liang, K. Wang, Q. Wu, W.-J. Sheng, Y.-X. Jia, *Organometallics* **2019**, *38*, 3927-3930; j) R.-X. Liang, R.-Z. Yang, R.-R. Liu, Y.-X. Jia, *Org. Chem. Front.* **2018**, *5*, 1840-1843; k) X. Li, B. Zhou, R.-Z. Yang, F.-M. Yang, R.-X. Liang, R.-R. Liu, Y.-X. Jia, *J. Am. Chem. Soc.* **2018**, *140*, 13945-13951; l) X. Qin, M. W. Y. Lee, J. S. Zhou, *Angew. Chem. Int. Ed.* **2017**, *56*, 12723-12726; *Angew. Chem.* **2017**, *129*, 12897-12900; m) R.-R. Liu, Y.-G. Wang, Y.-L. Li, B.-B. Huang, R.-X. Liang, Y.-X. Jia, *Angew. Chem. Int. Ed.* **2017**, *56*, 7475-7478; *Angew. Chem.* **2017**, *129*, 7583-7586; n) K. Douki, H. Ono, T. Taniguchi, J. Shimokawa, M. Kitamura, T. Fukuyama, *J. Am. Chem. Soc.* **2016**, *138*, 14578-14581; o) C. Shen, R.-R. Liu, R.-J. Fan, Y.-L. Li, T.-F. Xu, J.-R. Gao, Y.-X. Jia, *J. Am. Chem. Soc.* **2015**, *137*, 4936-4939; p) K.-J. Wu, L.-X. Dai, S.-L. You, *Org. Lett.* **2012**, *14*, 3772-3775.

[5] H. Chu, J. Cheng, J. Yang, Y.-L. Guo, J. Zhang, *Angew. Chem. Int. Ed.* **2020**, *59*, 21991-21996; *Angew. Chem.* **2020**, *132*, 22175-22180.

[6] In addition to indole, this CADA strategy could also be extended to OH- or NH-containing electron-rich aromatic substrates. For selected examples, see: a) X. Mu, H. Yu, H. Peng, W. Xiong, T. Wu, W. Tang, *Angew. Chem. Int. Ed.* **2020**, *59*, 8143-8147; *Angew. Chem.* **2020**, *132*, 8220-8224; b) L. Fan, J. Liu, L. Bai, Y. Wang, X. Luan, *Angew. Chem. Int. Ed.* **2017**, *56*, 14257-14261; *Angew. Chem.* **2017**, *129*, 14445-14449; c) L. Bai, Y. Yuan, J. Liu, J. Wu, L. Han, H. Wang, Y. Wang, X. Luan, *Angew. Chem. Int. Ed.* **2016**, *55*, 6946-6950; *Angew. Chem.* **2016**, *128*, 7060-7064; d) L. Yang, H. Zheng, L. Luo, J. Nan, J. Liu, Y. Wang, X. Luan, *J. Am. Chem. Soc.* **2015**, *137*, 4876-4879; e) K. Du, P. Guo, Y. Chen, Z. Cao, Z. Wang, W. Tang, *Angew. Chem. Int. Ed.* **2015**, *54*, 3033-3037; *Angew. Chem.* **2015**, *127*, 3076-3080; f) R.-Q. Xu, Q. Gu, W.-T. Wu, Z.-A. Zhao, S.-L. You, *J. Am. Chem. Soc.* **2014**, *136*, 15469-15472; g) S. Rousseaux, J. García-Fortanet, M. A. Del Aguila Sanchez, S. L. Buchwald, *J. Am. Chem. Soc.* **2011**, *133*, 9282-9285; h) J. García-Fortanet, F. Kessler, S. L. Buchwald, *J. Am. Chem. Soc.* **2009**, *131*, 6676-6677.

[7] a) G. L. Trammel, R. Kuniyil, P. F. Crook, P. Liu, M. K. Brown, *J. Am. Chem. Soc.* **2021**, *143*, 16502-16511; b) P. Yang, R.-Q. Xu, C. Zheng, S.-L. You, *Chin. J. Chem.* **2020**, *38*, 235-241; c) Z. Liu, J. Chen, H.-X. Lu, X. Li, Y. Gao, J. R. Coombs, M. J. Goldfogel, K. M. Engle, *Angew. Chem. Int. Ed.* **2019**, *58*, 17068-17073; *Angew. Chem.* **2019**, *131*, 17224-17229.

[8] V. Bhat, E. R. Welin, X. Guo, B. M. Stoltz, *Chem. Rev.* **2017**, *117*, 4528-4561.

[9] F. Ceccacci, G. Mancini, P. Mencarelli, C. Villani, *Tetrahedron: Asymmetry* **2003**, *14*, 3117-3122.

[10] a) Q. Wang, J. Hu, N. Zheng, *Org. Lett.* **2019**, *21*, 614-617; b) Y. Yu, J. Li, L. Jiang, J.-R. Zhang, L. Zu, *Angew. Chem. Int. Ed.* **2017**, *56*, 9217-9221; *Angew. Chem.* **2017**, *129*, 9345-9349; c) Y. Yu, G. Li, L. Jiang, L. Zu, *Angew. Chem. Int. Ed.* **2015**, *54*, 12627-12631; *Angew. Chem.* **2015**, *127*, 12818-12822.

[11] B. Zhou, H. Wang, Z.-Y. Cao, J.-W. Zhu, R.-X. Liang, X. Hong, Y.-X. Jia, *Nat. Commun.* **2020**, *11*, 4380.

[12] Deposition Number 2074943 (for **3aa**), 2120649 (for **4aa'**), and 2120650 (for **4am'**) contains the supplementary crystallographic data for this paper. These data are provided free of charge by the joint Cambridge Crystallographic Data Centre and Fachinformationszentrum Karlsruhe Access Structures service www.ccdc.cam.ac.uk/structures.